Articles

Biochemical Analysis of Catalytically Crucial Aspartate Mutants of Human Immunodeficiency Virus Type 1 Reverse Transcriptase†

Neerja Kaushik, Nisha Rege, Prem N. S. Yadav, Stefanos G. Sarafianos, Mukund J. Modak, and Virendra N. Pandey*

Department of Biochemistry and Molecular Biology, UMD-New Jersey Medical School, Newark, New Jersey 07103

Received February 15, 1996; Revised Manuscript Received May 29, 1996⊗

ABSTRACT: In order to clarify the role(s) of the individual member of the carboxylate triad in the catalytic mechanism of human immunodeficiency virus type 1 (HIV-1) reverse transcriptase, we carried out site-directed mutagenesis of D185, D186, and D110, followed by the extensive characterization of the properties of the individual mutant enzymes. We find that all three residues participate at or prior to the chemical step of bond formation. The incorporation pattern seen with phosphorothioate analogs of dNTP on both RNA−DNA and DNA−DNA template−primers indicated that D186 may be the residue that coordinates with the α-phosphate group of dNTP in the transition-state ternary complex. Further support for the role assigned to D186 was obtained by examination of the ability of the individual carboxylate mutants to catalyze the reverse of the polymerase reaction (pyrophosphorolysis). Mutants of D185 exhibited near-normal pyrophosphorolysis activity, while those of D186 were completely devoid of this activity. Thus, D185 appears to participate only in the forward reaction, probably required for the generation of nucleophile by interacting with the 3′-OH of the primer terminus, while D186 seems to be involved in both the forward and the reverse reactions, presumably by participating in the pentavalent intermediate transition state. Lack of any elemental effects during polymerization with mutant enzymes of residue D110, together with their inability to catalyze pyrophosphorolysis, suggest its probable participation in the metal-coordinated binding to the β-γ-phosphate of dNTP or PP_i in the forward and reverse reactions, respectively. A molecular model of the ternary complex based on these results is also presented.

Since the discovery of acquired immunodeficiency syndrome (AIDS), human immunodeficiency virus type 1(HIV-1)[1] reverse transcriptase has been the primary target in developing chemotherapeutic agents against HIV infection. HIV-1 RT, a virally encoded multifunctional DNA polymerase, is absolutely essential for the conversion of viral genomic RNA into double-stranded DNA that can then be integrated into the host genome (Barre-Sinoussi et al., 1983; Levy et al., 1984; Popovic et al., 1984). It is processed initially from the pol gene product as a 66-kDa polypeptide which is converted into a heterodimeric (66/51) form upon subsequent proteolytic cleavage (Dimarzo-Veronese et al., 1986; Lightfoote et al., 1986; Hansen et al., 1987; Leuthardt et al., 1988; Mous et al., 1988). This enzyme shares some common structural features with other DNA polymerases. These include a large cleft that accommodates the template−primer which is formed by a structurally similar three-dimensional motif consisting of the palm, thumb, and finger subdomains (Kohlstaedt et al., 1992; Jacobo-Molina et al., 1993). It has been subjected to extensive mutagenesis in order to identify the regions important for the polymerase function and those involved in conferring drug resistance/sensitivity (Larder et al., 1987, 1993; Boyer et al., 1992, 1994). Three carboxylate residues (D110, D185, and D186) were the first ones to be identified as being absolutely essential for the catalysis of the polymerase reaction (Larder et al., 1987; Lowe et al., 1991; Le Grice et al., 1991; Hostomsky et al., 1992). Furthermore, the carboxylate triad in the p66 subunit appeared to be catalytically important since mutation of the same in the p51 subunit did not result in the loss of the catalytic activity of HIV-1 RT (Le Grice et al., 1991; Hostomsky et al., 1992). These carboxylate residues have been proposed to participate in the metal coordination function required in the binding of deoxyribonucleotide substrates to the enzyme (Kohlstaedt et al., 1992; Jacobo-Molina et al., 1993; Pelletier et al., 1994). In addition, one

† This research was supported in part by a grant from the National Cancer Institute (CA72821) and by a Scholar award from the American Foundation for AIDS Research (to P.N.S.Y.).

* Address correspondence to this author.

⊗ Abstract published in *Advance ACS Abstracts,* August 15, 1996.

[1] Abbreviations: HIV-1 RT, human immunodeficiency virus type 1 reverse transcriptase; TdT, terminal deoxynucleotidyltransferase; IMAC, immobilized metal affinity chromatography; IDA−Sepharose, iminodiacetic acid−Sepharose; SDS−PAGE, sodium dodecyl sulfate−polyacrylamide gel electrophoresis; dNTP, deoxynucleoside triphosphate; dNTPαS, deoxynucleoside 5′-*O*-(1-thiotriphosphate); DTT, dithiothreitol; PMSF, phenylmethanesulfonyl fluoride; IPTG, isopropyl β-thiogalactopyranoside; poly(rA)·$(dT)_{18}$, polyriboadenylic acid annealed with $(thymidylic\ acid)_{18}$; poly(rC)·$(dG)_{18}$, polyribocytidylic acid annealed with $(deoxyguanylic\ acid)_{18}$; poly(rI)·$(dC)_{18}$, polyriboinosic acid annealed with $(deoxycytidylic\ acid)_{18}$; poly(dC)·$(dG)_{18}$, polydeoxycytidylic acid annealed with $(deoxyguanylic\ acid)_{18}$; WT, wild type; D185A, D185E, D186N, D186A, D186E, and D186N, substitution of aspartic acid with alanine, glutamic acid, and asparagine, respectively, at positions 185 and 186 of HIV-1 RT; D110A and D110S, substitution of aspartic acid with alanine and serine at position 110; TP, template−primer; E−TP, complex of enzyme with template−primer.

S0006-2960(96)00364-9 CCC: $12.00

Chart 1: Oligomeric DNA Template−Primers Used

37 meric self-annealing TP

```
   A   C
C          GCAGTCTTCTCC -3'
 T         CGTCAGAAGAGGATCCCTC  -5'
   C   A
```

47/18 mer TP

```
5' CTTCCATTCACACACTGC-3'
3'-GAAGGTAAGTGTGTGACGATGTCTGACCTTGTTTTTGTGACATTGAG-5'
```

18/26 mer TP

```
5'-CCGGCTAGTAGTACTAGT-3'
3'-GGCCGATCATCATGATCATTGTCATC-5'
```

of these metal-linked aspartates is speculated to interact with the 3′-O of the primer terminus nucleotide and help facilitate the nucleotidyltransferase reaction (Kohlstaedt et al., 1992). However, there is no experimental evidence to pinpoint the contribution of the individual carboxylates in binding interaction with the metal-complexed dNTP and the primer terminus. In order to clarify the participation of the individual aspartic acid in the above processes, we generated mutants of these residues and assessed their ability to interact with the normal and thiosubstituted dNTP substrates in the DNA polymerase reaction. Results implied that D186 was closest to the α-phosphoryl group of the metal-complexed nucleotide. Further clarification of the role of the individual carboxylate residues was assessed by examination of their participation in the pyrophosphorolysis reaction. Results of these investigations together with the experimental strategy forms the subject matter of the present investigation.

MATERIALS AND METHODS

Materials

Wild-type p66 and p51 subunits of HIV-1 RT were expressed and purified from the overproducing clones pET-28a-RT_{66} and pET-3a-RT_{51} respectively, in *Escherchia coli* BL-21 (DE−3) as described before (Sarafianos et al., 1995a,b; Pandey et al., 1996). Restriction endonucleases and DNA modifying enzymes were from Promega or Boehringer Mannheim. Homopolymeric templates and HPLC-purified dNTPs and deoxynucleoside 5′-*O*-(1-thiotriphosphate) analogs (dNTPαS, S_p isomer) were obtained from Pharmacia, while [γ-^{32}P]ATP, tritiated dNTPs, and [α-^{32}P]dNTPs were the products of Dupont−New England Nuclear Inc. Sequenase and other reagents were from U.S. Biochemical Corp. A self-annealing looped template−primer (see Chart 1) as well as other synthetic oligomeric primers were obtained from the Midland Certified Reagent Co. and were further purified by polyacrylamide gel electrophoresis (Maxam & Gilbert, 1980). An *in vitro* mutagen kit for mutagenesis was obtained from Bio-Rad. All other reagents were of the highest available purity grade and were purchased from Fisher, Millipore Corp., Boehringer Mannheim, and Bio-Rad. Terminal deoxynucleotidyltransferase used for the preparation of dideoxynucleotide-terminated 19-mer primer was purified from calf thymus glands (Pandey & Modak, 1987b).

Methods

Construction of Expression Plasmids and in Vitro Mutagenesis. The desired mutations were made on a dU-containing M13mp18 template (Kunkel et al., 1987) containing the region of the HIV-1 RT gene encoding the polymerase domain. As described previously (Sarafianos et al., 1995a,b; Pandey et al., 1996), this region was subcloned from pET-28a-RT51 in bacteriophage M13mp18, which contains unique *Kpn*I, *Bal*I, and *Sac*I restriction sites that are useful in subcloning. The mutagenesis, subcloning into high expression vectors, expression, and purification of the mutant and WT enzymes have been described before (Sarafianos et al., 1995a,b; Pandey et al., 1996). The different combinations of chimeric heterodimers were prepared by reconstitution of the separate subunits. Cell lysates of the different bacterial strains were mixed at the appropriate ratios, essentially following the protocol described by Le Grice et al. (1991). Protein concentrations were determined by using the Bio-Rad colorimetric kit as well as by spectrophotometric measurements using $\epsilon_{280} = 2.6 \times 10^5$ M^{-1} cm^{-1} (Kati et al., 1992).

Steady-State Kinetics of Polymerization. The kinetic studies were carried out at 25 °C as described before (Bryant et al., 1983; Majumdar et al., 1988, 1989; Pandey et al., 1994a; Desai et al., 1994) using homopolymeric poly(rA)·$(dT)_{18}$, poly(rC)·$(dG)_{18}$ and poly(dC)·$(dG)_{18}$ as the template−primers and dTTP or dGTP as the substrates. Template-primers were prepared by mixing equimolar amounts of template and primer at 20 mM concentrations. The reaction mixture contained 50 mM Tris-HCl, pH 7.5, 2 mM $MgCl_2$, 1 mM DTT, 100 mg of BSA/mL, and variable concentrations of both template−primer and [α-^{32}P]dNTP substrates. The concentration of enzyme used in the assay ranged from 5 nM for the wild-type enzyme to 200 nM for the carboxylate mutants. The reaction was initiated by the addition of $MgCl_2$ and terminated by the addition of 5% ice-cold TCA at desired time points. The TCA-precipitable materials were collected on Whatman GF/B filters and counted for radioactivity in liquid scintillation counter as described before (Pandey & Modak, 1987a). In some experiments, primer terminus was prelabeled at the 5′ position, annealed with the respective template, and used for the extension reaction. Samples (5 μL) were withdrawn at various time points and quenched with an equal volume of DNA gel loading solution [0.25% SDS, 35 mM EDTA, 90% deionized formamide, and 0.02% (w/v) each of bromophenol blue and xylene cyanol]. The samples were heated at 100 °C for 3 min and resolved by electrophoresis on 16% denaturing polyacrylamide gels followed by autoradiography. The radioactive bands were either cut out from the gel and counted for Cerenkov counts per minute or quantitated by the scanning and integration of the bands on the autoradiogram. Velocities for each substrate concentration were fit to the Michaelis−Menten equation and least-squares lines were drawn for the Lineweaver−Burk plots. K_m and V_{max} were calculated graphically; k_{cat} was calculated from the equation $V_{max} = k_{cat}[E]$.

Cross-Linking of Enzyme to Template−Primer. We have used poly(rA)·(5′-^{32}P-$(dT)_{18}$ as well as a self-annealing 5′-^{32}P-labeled 37-mer template−primer for the binding studies (see Chart 1). The oligomers were 5′-labeled using [γ-^{32}P]-ATP and T4 polynucleotide kinase according to the standard protocol (Ausubel et al., 1987). The labeled oligomers were purified on a NAP-10 column (Pharmacia) and adjusted to the required specific activity with the unlabeled oligomer. Poly(rA)·5′-^{32}P-$(dT)_{18}$ was prepared by annealing labeled $(dT)_{18}$ and poly(rA) in a molar ratio of 3:1. For cross-linking,

512 nM enzyme and 15 nM labeled TP (75 000 cpm /pmol) with respect to the primer termini were incubated on ice for 10 min in a solution containing 50 mM Tris-HCl, pH 7.5, 1 mM DTT, 2 mM $MgCl_2$, 75 mM NaCl, and 5% glycerol in a final volume of 50 μL. The mixture was exposed to UV irradiation and the TP cross-linked enzyme species were resolved by electrophoresis on SDS−polyacrylamide gels and the extent of cross-linking was quantitated by excising the radioactive bands and measuring the Cerenkov counts associated with them.

Effect of Thiophosphoryl Substitution at the α*-Phosphoryl Group of dNTPs on the Polymerase Activity.* The effects of the thiophosphoryl-substituted dNTP on the polymerase activity of the carboxylate mutants were determined with RNA−DNA [poly(rA)·$(dT)_{18}$ and poly(rC)·$(dG)_{18}$] and DNA−DNA template−primers [47/18-mer heteropolymeric DNA and poly(dC)·$(dG)_{18}$] together with the respective deoxynucleoside 5′-*O*-(1-thiotriphosphate) (dNTPαS) substrates. The dNTPαS analogs were pure S_p diastereomers and were used at 50 μM concentration with homopolymeric TPs and 200 μM (50 μM each) with heteropolymeric TPs. The oligomeric primers were 5′-^{32}P-labeled and purified by electrophoresis on 16% polyacrylamide−8 M urea gels (Maxam & Gilbert, 1980). The purified ^{32}P-labeled oligomer was annealed with a 5-fold excess of the respective templates. A typical reaction contained 5 nM labeled template−primer (0.5×10^6 Cerenkov cpm/pmol), 50 mM Tris-HCl, pH 7.5, 1 mM DTT, 100 μg/mL BSA, 50 μM either normal dNTP or its thiophosphoryl analog (dNTP αS), and 200 nM mutant enzyme in a final volume of 60 μL. All reactions were carried out at 25 °C, and 5-μL samples were removed at different time intervals and quenched with an equal volume of the DNA gel loading solution. The samples were heated at 100 °C for 3 min and the products were resolved by electrophoresis on a denaturing 16% polyacrylamide−8 M urea gel. The labeled products were detected by autoradiography.

Cross-Linking of Enzyme to Oligophosphorothioate Primer−Template. To assess the binding affnity for the phosphorothioate nucleotide-containing template−primer, we have used a 22/26-mer heteromeric template−primer with four sulfur-substituted nucleotides from the 3′ terminus of the primer strand. For this, the 5′-^{32}P-labeled 18/26-mer template−primer was extended to a 22/26-mer by incorporating four thionucleotides using the Klenow fragment and dNTPαS (Pandey et al., 1996). The reaction mixture (30 μL) contained 50 mM Tris-HCl, pH 7.5, 1 mM DTT, 100 μg of BSA/mL, 2 mM $MgCl_2$, 250 nM 5′-^{32}P-labeled 18/26-mer (75 000 cpm/pmol), 50 nM exonuclease-deficient Klenow fragment, and 20 μM each of the phosphorothioate analogs of dATP and dCTP. The reaction mixture was incubated at room temperature for 60 min and terminated by the addition of 10 mM EDTA followed by heating at 65 °C for 5 min and slow cooling to room temperature. For comparison the 5′-^{32}P-labeled 18/26-mer was extended to a 22/26-mer by incorporation of four nonphosphorothioate nucleotides under similar conditions. For cross-linking, 15 nM phosphorothioate and nonphosphorothioate 5′-^{32}P-labeled 22/26-mer and 512 nM WT HIV-1 RT or its mutant derivative was UV-irradiated and the extent of cross-linking was determined as described before.

Measurements of Pyrophosphorolysis Reaction. Pyrophosphorolysis activity of each carboxylate mutant was estimated by analyzing the products of the reaction on denaturing polyacrylamide gels. The DNA substrate was prepared by annealing 5′-^{32}P-labeled $(dT)_{18}$ with poly(rA) at equimolar concentrations. The reaction mixture contained 50 mM Tris-HCl, pH 7.5, 1 mM DTT, 100 μg of BSA/mL, 5 mM $MgCl_2$, 5 nM of poly(rA)·5′-^{32}P-$(dT)_{18}$ (0.5×10^6 Cerenkov cpm/pmol), 500 μM sodium pyrophosphate and 200 nM mutant enzyme in a final volume of 6 μL. Since Mg·PP_i has a very high stability constant (250 000 M^{-1}; James & Morrison, 1966), we find that by increasing the concentration of PP_i, a substantial amount of Mg·PP_i is precipitated in the reaction. Furthermore, the higher concentration of Mg·PP_i (<2 mM) is inhibitory to the reverse reaction catalyzed by the WT enzyme. We observed that the extent of pyrophosphorolysis products generated with the WT enzyme at 0.5 mM and 1.5 mM Mg·PP_i was similar but was significantly reduced at or above 2 mM Mg·PP_i. The reactions were carried out at 25 °C for 60 min and quenched with an equal volume of DNA gel loading solution. The samples were heated at 100 °C for 3 min and resolved by electrophoresis on a denaturing 16% polyacrylamide−8 M urea gel. The labeled products were detected by autoradiography. In some of the experiments pyrophosphorolysis activity was estimated by using poly(47-mer)·5′-^{32}P-(19-mer) containing dideoxythymidine monophosphate (ddTMP) as the terminal primer nucleotide. The dideoxy-terminated 19-mer primer was prepared by terminal deoxynucleotidyltransferase (TdT) as follows: 10 nmol of polyacrylamide gel-purified 18-mer primer was incubated with 20 nmol of ddTTP in a reaction mixture containing 50 mM Tris-HCl, pH 7.8, 1 mM DTT, 100 μg of BSA/mL, 2.5 mM $MgCl_2$, and 2 μg of calf thymus TdT in a final volume of 100 μL. The reaction mixture was incubated at room temperature for 16 h and terminated by heating at 75 °C for 5 min. The dideoxy-terminated 19-mer was purified on a Sep-Pak QMA cartridge (Waters Division, Millipore). One hundred picomoles of the purified 19-mer primer was labeled at the 5′ terminus, purified by electrophoresis on a 16% polyacrylamide−8 M urea gel, and annealed with a 5-fold excess of 47-mer template.

RESULTS

Construction and Purification of the Mutant Enzymes. The mutants of the catalytic carboxylate triad (D110, D185, and D186) of HIV-1 RT were constructed and expressed in *E. coli* as described before (Sarafianos et al., 1995a,b; Pandey et al., 1994a; Desai et al., 1994). Mutants of D185 and D186 were generated by replacing Asp with Ala, Glu, or Asn, while D110 was replaced with Ala or Ser. The purified heterodimeric (p66/p51) enzyme preparations were found to be more than 95% pure. The level of their expression, solubility, yield, and the chromatographic characteristics were identical with those of the wild-type enzyme, suggesting that substitution at these positions did not cause any perturbation in the enzyme structure. All the mutants were RNase H positive and showed a heat inactivation pattern identical to that of the WT HIV-1 RT (results not shown), thus providing additional evidence that these mutations had not altered the folded structure of the protein.

Kinetic Parameters of the Mutant Enzyme. The kinetic characterization of the polymerase reaction, using different template−primers, was carried out using purified enzymes, and results are summarized in Table 1. As seen from the

Table 1: Kinetic Parameters of the Carboxylate Mutants[a]

	poly(rA)·(dT)$_{18}$/dTTP			poly(rC)·(dG)$_{18}$/dGTP			poly(dC)·(dG)$_{18}$/dGTP		
enzyme	$K_{m_{dTTP}}$ (μM)	k_{cat} (s^{-1})	k_{cat}/K_m (M^{-1} s^{-1})	$K_{m_{dGTP}}$ (μM)	k_{cat} (s^{-1})	k_{cat}/K_m (M^{-1} s^{-1})	$K_{m_{dGTP}}$ (μM)	k_{cat} (s^{-1})	k_{cat}/K_m (M^{-1} s^{-1})
WT	2.2	1.7×10^{-1}	7.8×10^4	2.60	2.6×10^{-1}	1.0×10^5	1.90	2.9×10^{-1}	1.5×10^5
D110A	10.2	2.5×10^{-4}	24.0	10.20	2.5×10^{-4}	24.0	1.30	4.9×10^{-4}	376.0
D110S	24.0	5.9×10^{-4}	24.0	4.00	1.0×10^{-4}	25.0	2.90	2.5×10^{-2}	8.7×10^3
D185A	5.3	2.3×10^{-5}	43.0	5.30	2.3×10^{-4}	43.0	3.50	7.7×10^{-5}	22.0
D185E	31.8	2.7×10^{-4}	8.0	0.30	3.9×10^{-5}	130.0	7.20	1.0×10^{-4}	13.0
D185N	24.5	3.5×10^{-4}	14.0	3.80	1.3×10^{-4}	34.0	3.80	1.3×10^{-4}	34.0
D186A	5.5	1.7×10^{-5}	31.0	2.00	9.4×10^{-5}	47.0	1.30	8.2×10^{-5}	63.0
D186E	8.6	1.0×10^{-4}	11.0	6.50	1.9×10^{-4}	29.0	4.40	1.9×10^{-4}	43.0
D186N	16.5	4.2×10^{-4}	25.0	3.80	1.3×10^{-4}	34.0	2.60	6.0×10^{-4}	230.0

[a] The steady-state kinetic parameters for the WT HIV-1 RT and its carboxylate mutant derivatives were measured with the indicated template−primers and corresponding dNTP substrates as described under Materials and Methods.

table, the different aspartate mutants exhibited varying degrees of affinity for dNTP substrates depending upon the template−primer used. With poly(rA)·(dT)$_{18}$, the affinity of D110 mutants for dTTP substrate reduced by 5−12-fold (increase in K_m) but was unchanged for dGTP on poly(dC)·(dG)$_{18}$. Similarly, mutants of D185 and D186 exhibited lower affinity for dTTP on poly(rA)-directed extension reaction while very little change in the affinity for dGTP was observed with poly(rC)- or poly(dC)-directed reactions. The k_{cat} of the polymerase reaction of D110A mutant enzyme was 600- and 1000-fold lower than the WT enzyme for RNA and DNA template-directed reactions, respectively. In contrast, D → S substitution at the 110 position selectively inactivated the RNA-directed DNA synthesis but significantly retained the DNA-directed catalysis. As shown in the table, with D110S, a 300- and 2600-fold reduction in k_{cat} was observed with poly(rA) and poly(rC) templates, respectively, while only a 10-fold reduction was noted with poly(dC)-directed reactions. The extent of reduction in k_{cat} with D185 and D185 mutants ranged between 480- and 6600-fold with different template−primers. Among the carboxylate mutants, both D110A and D110S showed a consistently higher efficiency of polymerization (k_{cat}/K_m) selectively with DNA template-directed reactions. These results provide a subtle clue that Asp 110 may not be absolutely essential for DNA-directed synthesis but may be predominantly utilized in RNA-directed DNA synthesis.

Formation of E−TP Binary Complexes. The large decrease in k_{cat} of polymerization seen with the individual mutants of the carboxylate triad prompted us to ascertain whether these mutations adversely affect the binding of the template−primer. A direct photochemical cross-linking of RNA−DNA template−primer [poly(rA)·5′-^{32}P-(dT)$_{18}$] and DNA−DNA template−primer (47/18-mer) to the mutant and the wild-type enzymes was performed by UV irradiation of the desired E−TP complexes under standard conditions (Pandey et al., 1987, 1994b) and the extent of E−TP covalent complex formed was analyzed by SDS−polyacrylamide gel electrophoresis. Results shown in Figure 1 indicate no change in the E−TP binary complex formation with the individual mutants of the triad.

Rate-Limiting Step of the Reaction. Since all mutant enzymes of the carboxylate triad exhibited a substantial reduction in k_{cat} but no change in TP binding, we carried out further analyses to identify whether the rate-limiting step of the reaction with these mutant enzymes preceded or followed the chemical step, i.e., phosphodiester bond formation. Using poly(rA)·5′-^{32}P-(dT)$_{18}$ as the template−primer

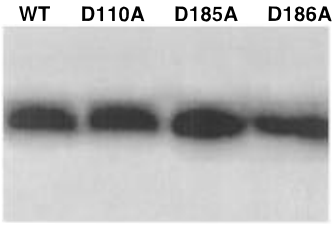

FIGURE 1: Qualitative assessment of template−primer binding affinity of carboxylate triad mutants by photochemical cross-linking. WT HIV-1 RT and its carboxylate mutant derivatives (512 nM) were incubated on ice with poly(rA)·(dT)$_{18}$, template−primer at a concentration of 15 nM in standard solution. The mixtures were irradiated in the UV-Spectrolinker and subjected to SDS−PAGE and autoradiography as described before (Pandey et al., 1994b).

and an excess of the individual mutant enzyme, a time course of dTMP incorporation was performed and the reaction products were analyzed on polyacrylamide−urea gels. It was reasoned that if the extension (dT)$_{18}$ is linear with time, then the rate-limiting step must be at or preceding bond formation. Figure 2 shows the time course of reaction products of the D186E mutant. As can be seen from the figure, the extension of 18-mer primer to 19-, 20-, and 21-mer products is linear with time. Similar results were obtained for D186N, D185E, D185N, and D110S mutants (data not shown) which suggest that the rate-limiting step with these mutant enzymes occurs before or at the point of phosphodiester bond formation. For comparison, the extension of (dT)$_{18}$ by a mutant enzyme (R72A) of HIV-1 RT that stalls on DNA following the addition of the first nucleotide is shown in panel B of Figure 2. This is in contrast to the extension of (dT)$_{18}$ by the R72A mutant of HIV-1 RT, which is nonlinear with time, suggesting that the rate-limiting step for this mutant may be after phosphodiester bond formation (Sarafianos et al., 1995).

Incorporation of αTTPαS. The possibility of the chemical step (phosphodiester bond formation) being the rate-limiting step was examined by comparing the ability of the individual mutant enzymes to catalyze the incorporation of dTMP vs dTMPαS into poly(rA)·(dT)$_{18}$. A mutant enzyme of a particular residue displaying a significant difference in the utilization of normal vs phosphorothioate analog of dNTP, also known as a sulfur elemental effect, implies reactivity of the side chain of that residue with the α-phosphate of dNTP. Figure 3 shows the products formed with dTTP and dTTPαS as a function of time with three mutants each of D185 and D186. As shown in the figure (Figure 3A), with D185A, no sulfur elemental effect could be discerned for lack of catalysis. However, both D185E and D185N showed

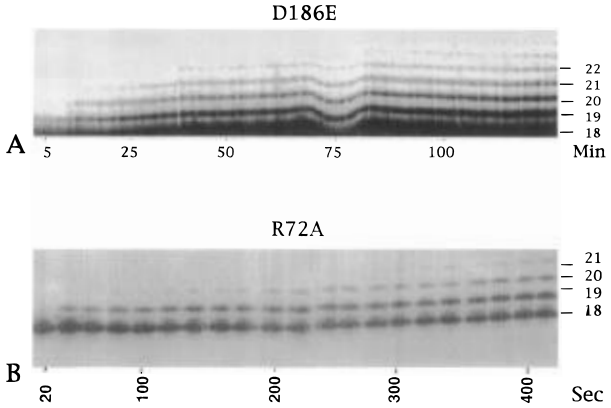

FIGURE 2: (A) Time course of incorporation of dTTP by D186E mutant. The 5′-^{32}P-labeled $(dT)_{18}$ annealed with poly(rA) was used to assess the time course of extension of $(dT)_{18}$ to $(dT)_{18+1}$ and $(dT)_{18+2}$ by D186E mutant enzyme. The mutant enzyme (200 nM) was incubated with 5 nM labeled template−primer (10^6 Cerenkov cpm/pmol) in the presence of 100 μM dTTP as described under Materials and Methods. Aliquots were withdrawn at the indicated time points and the reaction products were analyzed on denaturing 16% polyacrylamide−8 M urea gels followed by autoradiography on Kodak X-ray film. (B) Time course of incorporation of dTTP by the R72A mutant of HIV-1 RT. Arg → Ala substitution at 72 position affects the reaction step following the phosphodiester bond formation, and therefore, incorporation of dTMP is found to be nonlinear with time.

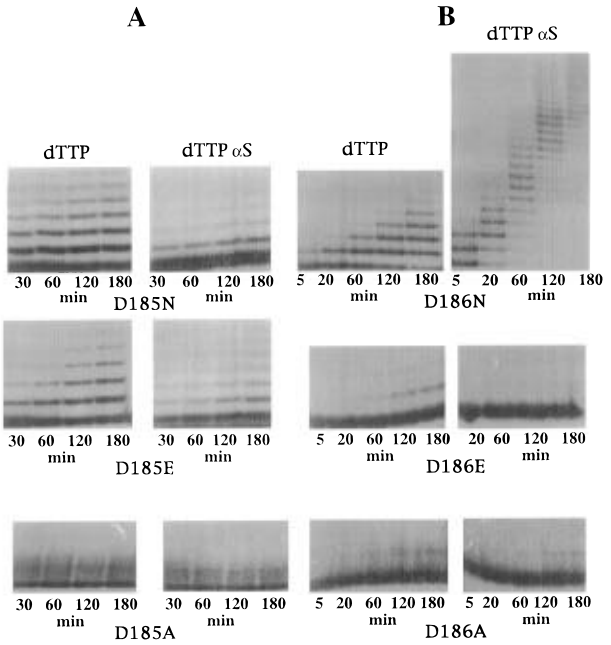

FIGURE 3: Incorporation of dNTP and dNTPαS on RNA−DNA template−primer by carboxylate mutant derivatives of WT HIV-1 RT. Individual mutant derivatives (200 nM) of either D185 (A) or D186 (B) were incubated with 5 nM poly(rA)·5′-^{32}P-$(dT)_{18}$ (0.5×10^6 Cerenkov cpm/pmol) in the presence of 50 μM of dTTP or αTTPαS as described under Materials and Methods. Aliquots were withdrawn at indicated time points and analyzed on denaturing polyacrylamide gels as described above. As indicated, the left panels in both A and B show the incorporation of dTTP, while the right panels show the incorporation of αTTPαS.

only a slight decrease in the rate of incorporation of αTTPαS as compared to dTTP. In the case of mutants of D186, no elemental effect was seen with the D186A mutant as the extent of addition of dTTP and αTTPαS remained nearly identical (Figure 3B). In contrast, D186E and D186N exhibited a mixed sulfur elemental effect. The incorporation

Table 2: Rate of Incorporation of dTTP and αTTPαS by Carboxylate Mutants of HIV-1 RT[a]

	rate of incorporation[b]		
enzyme	dTTP (min^{-1})	αTTPαS (min^{-1})	ratio dTTP/αTTPαS
D185A	3.0×10^{-4}	2.7×10^{-4}	1.1
D185E	7.9×10^{-3}	3.2×10^{-3}	2.5
D185N	6.2×10^{-3}	1.2×10^{-3}	5.1
D186A	3.3×10^{-3}	2.9×10^{-3}	1.1
D186E	7.8×10^{-3}	2.1×10^{-4}	37.1
D186N	6.6×10^{-3}	3.4×10^{-2}	0.2
D110A	2.5×10^{-3}	2.3×10^{-3}	1.0
D110S	6.9×10^{-3}	1.9×10^{-3}	3.6

[a] The first-order rate constants were determined from an experiment of the type shown in Figure 2. A plot of the log of $(dT)_{18}$ primer remaining unutilized versus time gave the slope equal to the apparent first-order rate constant for the incorporation of dTMP. [b] Please note that the values for these rates may have a considerable degree of error due to the extremely low level of incorporation.

of αTTPαS is significantly reduced with the D186E mutant, while it is stimulated with D186N (Figure 3B). These results strongly suggest that the D186 may be the major interacting residue with the α-phosphate of dNTP. The extent of elemental effect seen with the mutants of D110 was much smaller as compared to the mutants of D186, suggesting it to be far from the α-phosphate of the dNTP substrate (Table 2).

In order to evaluate the extent of the sulfur elemental effect on each of the carboxylate mutants, pre-steady-state rate constants for incorporation of dTTP and its phosphorothioate analog were determined. As shown in Table 2, the ratio of αTTP/dTTPαS utilization by D185E and D185N was 2.5 and 5.1, respectively whereas the ratio for corresponding mutants of D186 was 37 and 0.2. Similar results were obtained for the incorporation of dCTP and dCTPαS with poly(rI)·$(dC)_{18}$ template−primer (results not shown). The D186 mutants (D186E and D186N) showed a pronounced sulfur elemental effect with all the template−primers.

Since the above experiments were carried out with homopolymeric RNA−DNA and DNA−DNA template−primers, it was essential to determine whether a similar pattern exists with the natural DNA−DNA template−primer. Thus, using a heterooligomeric 47/18-mer template−primer, we determined the incorporation pattern of dNTP versus dNTPαS by each of the mutants. Figure 4 represents results obtained with mutants of D185 and D186. The levels of incorporation of both normal dNTPs and dNTPαS by mutant derivatives of D185 (D185A, D185E, and D185N) were much higher (Figure 4A) than those seen with the mutants of D186 (D186A, D186E, and D186N) (Figure 4B). Most interestingly, the D185A mutant which is almost inactive with RNA template is also capable of extending the primer significantly, while D186A could barely add a single nucleotide during the entire incubation period. The sulfur elemental effect was found to be much more prominent with D186E and D186N than with the mutant derivatives of D185. Most curious results were obtained with D110 mutants, especially the D110S. This mutant derivative is significantly active with poly(dC)·$(dG)_{18}$ but is unable to catalyze reaction with the 47/18-mer template−primer. This could be due to specific structural differences in the homopolymeric and heteropolymeric template−primers. Due to the total lack of catalysis with the 47/18-mer template−primer, we could not assess the sulfur elemental effect on these mutants.

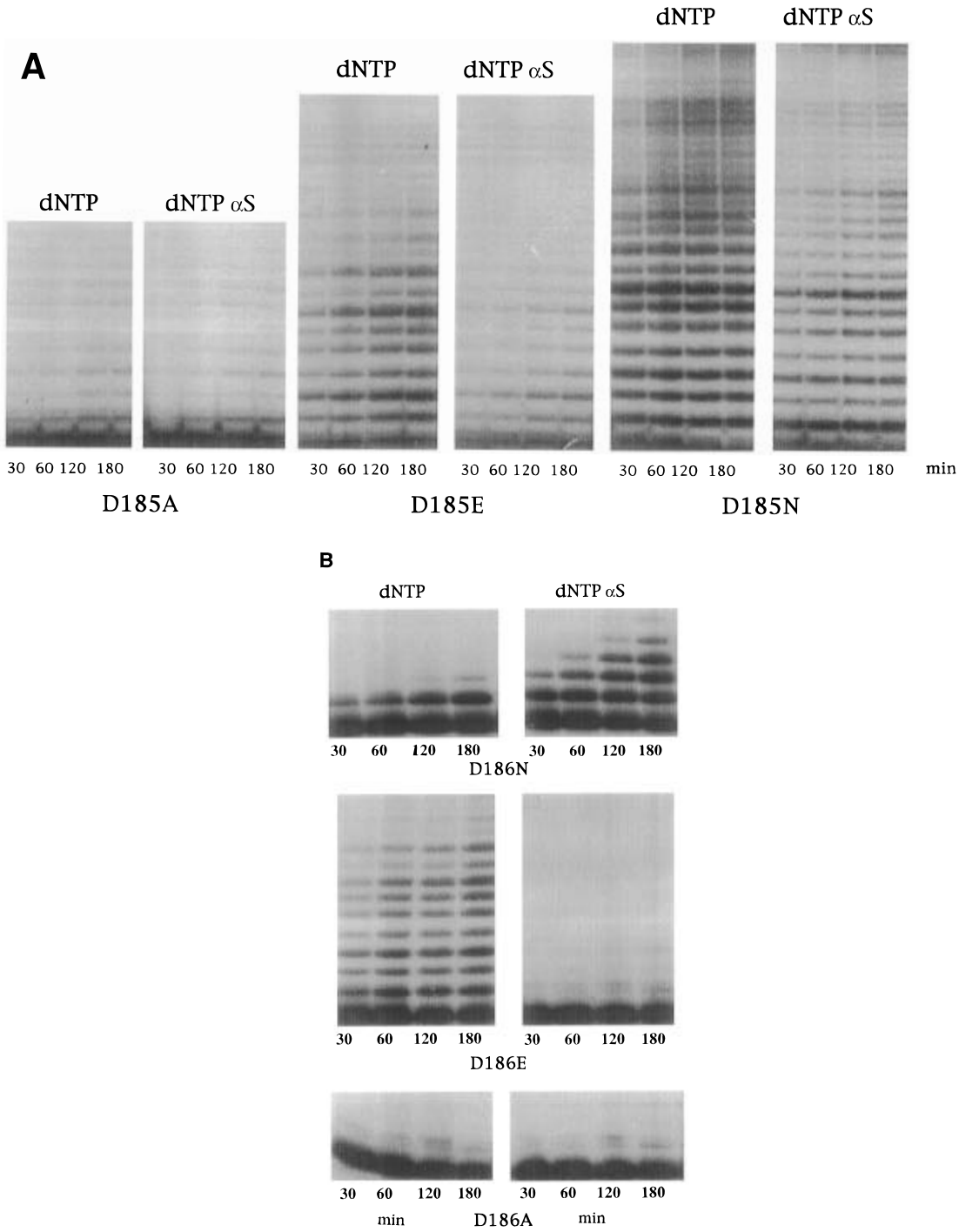

FIGURE 4: Incorporation of dNTP and dNTPαS on DNA−DNA template−primer by carboxylate mutant derivatives of WT HIV-1 RT. The 5′-^{32}P-labeled heteromeric 18-mer primer annealed with a 5-fold excess of heteromeric 47-mer template was used in this experiment. Individual mutant derivatives (200 nM) of D185 (A) or D186 (B) were incubated with 5 nM labeled template−primer in the presence of either all four dNTPs or their phosphorothioate analogs each at 50 μM concentration as described under Materials and Methods. Samples were aliquoted at indicated time points and analyzed as described before. As indicated, the left panels in both A and B show the incorporation of dNTP, while the right panels show the incorporation of dNTPαS.

Since the sulfur elemental effect was assessed under processive conditions, it was essential to determine whether the observed elemental effect with D186 mutants is due to the altered binding affinity for the template−primer following the incorporation of phosphorothioate nucleotide(s). We have therefore used a 5′-^{32}P-labeled 18/26-mer heteromeric template−primer with four sulfur-substituted nucleotides at the 3′ primer terminus to determine the binding affinity by photoaffinity cross-linking. The cross-linking was carried out at a subsaturating concentration of the template−primer (15 nM) in order to detect even small changes in the binding affinity. It was observed that none of the mutants showed any reduction in the cross-linking with this template−primer. In contrast, a slightly increased affinity for the phosphorothioate primer was observed with the WT and the carboxylate mutant derivatives as compared to the nonphosphorothioate 22/26-mer TP (Figure 5). This also confirms an earlier report that the affinity of HIV-1 RT for phosphorothioate oligonucleotide primer template is greater than that for the normal template−primer (Majumdar et al., 1989).

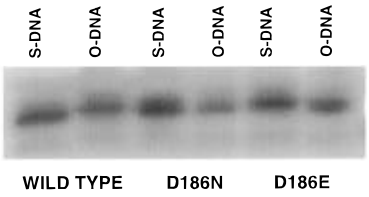

FIGURE 5: Binding of oligophosphorothioate primer-template to wild-type HIV-1 RT and D186 carboxylate mutants. WT HIV-1 RT or its mutant derivatives (512 nM) were incubated on ice with 15 nM 5′-^{32}P-labeled 22/26-mer template−primer with or without four 3′-terminal phosphorothioate nucleotides on the primer strand in standard solution. The 5′-^{32}P-labeled 22/26-mer template−primer with or without sulfur nucleotides, was prepared as described under Materials and Methods. The mixtures were irradiated in the UV-Spectrolinker and subjected to SDS−PAGE and autoradiography as described before (Pandey et al., 1994b).

The catalytic efficiency of HIV-1 RT was also shown to be 12-fold greater with primer containing multiple sulfur nucleotides due to the increase in the affinity for the template−primer as well as an increase in the processivity of DNA synthesis (Majumdar et al., 1989). This may well explain the positive sulfur elemental effect observed with the D186N mutant.

Pyrophosphorolysis Activity of the Carboxylate Mutants. Since the polymerase activity of HIV-1 RT is abolished by a conservative or nonconservative mutation of any one member of the catalytic aspartate triad, the effect of these mutations on the reverse of the polymerase reaction (pyrophosphorolysis) was assessed to confirm the suspected participation of the individual residues. Pyrophosphorolysis is the reverse of polymerase reaction, where the primer length is sequentially reduced in the presence of PP_i, resulting in the generation of dNTP. It was expected that the catalytic residue involved in the phosphodiester bond formation in the forward polymerase reaction must also be involved in the bond breakage in the reverse (pyrophosphorolysis) reaction. We used 5′-^{32}P-$(dT)_{18}$ annealed with poly(rA) as the template−primer to assess the degradation of 5′-^{32}P-$(dT)_{18}$ by these mutants in the presence of PP_i. The results shown in Figure 6A indicate that mutants of D186 and D110 are devoid of pyrophosphorolysis activity, whereas mutants of D185 are capable of catalyzing this reaction. Similar results were also obtained with poly(rI)·5′-^{32}P-$(dC)_{18}$ (Figure 6B) and with 47/18-mer DNA−DNA template−primer (Figure 6C). These observations clearly suggest that D185 is not the catalytic residue for the reverse reaction with both RNA−DNA and DNA−DNA template−primers.

Since, in the molecular model of HIV-1 RT/DNA/dNTP prepolymerase ternary complex, D185 has been postulated to be involved in metal coordination with the 3′-O of the primer terminus, we were curious whether primer lacking 3′-OH would be accepted in the pyrophosphorolysis reaction by the WT and mutant enzymes. We therefore repeated the pyrophosphorolysis assay with 5′-^{32}P-labeled dideoxy-terminated $(dT)_{18}$ annealed with poly(rA). Results shown in Figure 7 show that pyrophosphorolysis is independent of 3′-OH on the primer terminus, as the dideoxy-terminated primer are competent substrates for pyrophosphorolysis. Furthermore, mutants of D186 exhibited loss of this activity while mutants of D185 were found to be significantly active, thus confirming the noninvolvement of this residue in the reverse reaction.

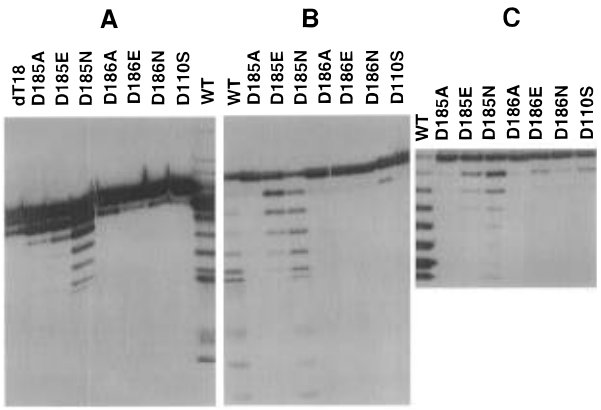

FIGURE 6: Pyrophosphorolysis reaction catalyzed by mutants of the carboxylate triad of HIV-1 RT. Three different substrates representing RNA−DNA [poly(rA)·$(dT)_{18}$ and poly(rI)·$(dC)_{18}$] and DNA−DNA (47/18-mer) template−primers were used for this experiment. The gel-purified 5′-^{32}P-labeled oligomeric primer annealed with the respective template was incubated with the mutant derivatives in the presence of 500 μM sodium pyrophosphate as described under Materials and Methods. Each panel show the electrophoretic separation of the reaction products after 60 min of incubation at 25 °C. Panel A, with poly(rA)·$(dT)_{18}$; panel B, with poly(rI)·$(dC)_{18}$; panel C, with 47/18-mer.

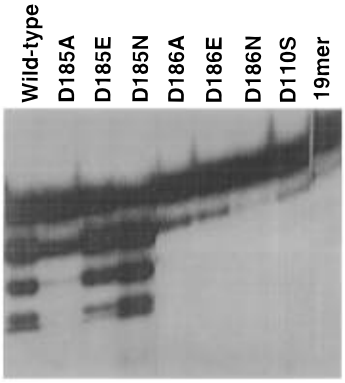

FIGURE 7: Effect of template−primer with 3′-dideoxy terminated primer strand on the pyrophosphorolysis reaction catalyzed by the mutants of carboxylate triad. The 18-mer primer was converted to a 19-mer by using ddTTP and calf thymus TdT as described under Materials and Methods. The 19-mer primer was then labeled with ^{32}P at the 5′-terminus and purified by denaturing 16% polyacrylamide−8 M urea gel electrophoresis (Maxam & Gilbert, 1980). The gel-eluted labeled 19-mer was annealed with the 47-mer template and used for pyrophosphorolysis reaction as described in Figure 5. The reaction products were resolved on denaturing polyacrylamide gels as described before.

DISCUSSION

Earlier mutational studies have shown that mutations of carboxylate residues D110, D185, and D186 can severely impair the catalytic activity of HIV-1 RT (Larder et al., 1989; Boyer et al., 1992; Wakefield et al., 1992). Subunit-specific mutagenesis of these residues further demonstrated that the carboxylates resident in the p66 subunit are essential for the catalytic activity (Le Grice et al., 1991; Hostomsky et al., 1992). However, the precise role played by the individual carboxylates in the catalytic function has remained unknown. A comparison of the three-dimensional structures of the Klenow fragment with that of HIV-1 RT has revealed that despite their weak sequence homology, the catalytically important carboxylate triad can be superimposed in both enzymes (Yadav et al., 1994; Kohlstaedt et al., 1992). The functional equivalence of the carboxylate triad residues D185,

D186, and D110 of HIV-1 RT with D882, E883, and D705 of the Klenow fragment, respectively, has been experimentally established as mutations of these residues in the Klenow fragment severely reduce the polymerase activity of the mutant enzymes (Polesky et al., 1990, 1992). Since D882, E883, and D705 residues have been observed to bind the divalent metal ions in the Klenow fragment [Beese and Steitz, unpublished observation cited in Kohlstaedt et al., (1992)] and have also been proposed to participate in the metal coordination function required in the binding of the deoxyribonucleotide substrates and 3′-O of the primer terminus to the enzyme, a similar role has been postulated for the corresponding D185 in HIV-1 RT (Patel et al., 1995). In order to clarify the interaction of the individual aspartic acid residues with the phosphoryl group of Mg·dNTP substrate and to determine their role in catalysis, we generated mutants of D185 and D186 by replacing them with Ala, Glu, or Asn, while D110 was replaced with Ala or Ser. The mutant enzymes were purified to homogeneity and characterized for their kinetic properties with respect to polymerase reaction with different template−primers. All the mutants exhibited most drastic reduction in k_{cat} with poly(rC)·$(dG)_{18}$, followed by poly(rA)·$(dT)_{18}$ and poly(dC)·$(dG)_{18}$ template−primers. Among three carboxylates, D186 mutants showed the most severe reduction in k_{cat} as compared to D185 and D110. Interestingly, D110A and D110S consistently showed a higher efficiency of polymerization (k_{cat}/K_m) with DNA−DNA template−primer as compared to RNA−DNA template−primer. This observation may be indicative of subtle changes in the utilization of metal-coordinating carboxylates in DNA synthesis directed by DNA versus RNA templates. It is likely that to some extent a neighboring residue, D113, may be able to substitute or complement metal coordination function of D110, although no experimental evidence exists for this notion.

The time course of the reactions for the extension of $(dT)_{18}$ with all carboxylate mutants have shown that the rate-limiting step occurs at or before the chemical step (phosphodiester bond formation). DNA affinity labeling and steady-state kinetic studies have ruled out the possibility that the DNA or dNTP binding step in the E−DNA−dNTP ternary complex is the rate-limiting step. To determine which of the carboxylates is involved in coordinating with the α-phosphoryl group of Mg·dNTP in the transition state, we compared the rates of addition of a deoxynucleoside 5′-*O*-(1-thiotriphosphate) analog (dNTPαS) with that of normal dNTP substrate by the individual mutant enzymes. We observed that D186E and D186N show a pronounced elemental effect while D185A, D186A, D110A, and D110S do not (Figures 3 and 4; Table 2). For D185E and D185N, the observed elemental effect was significantly lower as compared to the D186E and D186N mutants. Most interestingly, the rate of incorporation of the α-thio-substituted dNTP increased with the D186N mutant, suggesting a positive elemental effect on this mutant. Similar results were also obtained for the incorporation of dCTP, dGTP, and their phosphorothioate analogs on their respective template−primers, poly(rI)·$(dC)_{18}$, poly(rC)·$(dG)_{18}$, and poly(dC)·$(dG)_{18}$. In all cases the elemental effect was prominently seen with the D186 mutants. Similar elemental effects have also been noted with D882 mutants of the Klenow fragment (Polesky et al., 1992).

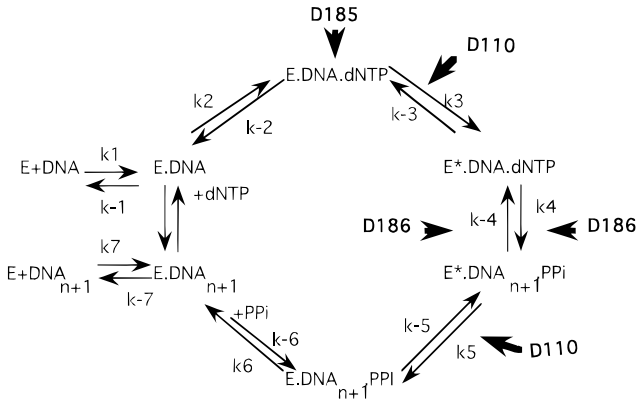

FIGURE 8: Postulated role of D110, D185, and D186 in the kinetic scheme of DNA polymerization catalyzed by HIV-1 RT. In this scheme we propose that D110 stabilizes the transition-state ternary complexes by interacting with the $\beta-\gamma$-phosphate of dNTP at k_3/k_{-3} and with PP_i at k_5/k_{-5}, respectively. This postulation is conceived by the fact that mutants of this residue do not exhibit a sulfur elemental effect and are devoid of both polymerase and pyrophosphorolysis activities. D185 is proposed to be involved in binding to dNTP as well as the 3′-O of the primer terminus only at the initial stage at k_2/k_{-3} step, as judged by loss of polymerase activity without any significant reduction in the pyrophosphorolysis activity. D186 is proposed as the catalytic residue interacting with the α-phosphate of dNTP or diester phosphate of the ultimate primer nucleotide in the transition-state ternary complexes at the k_3/k_{-3} and k_5/k_{-5} steps and thus leading to subsequent bond formation/cleavage at the k_4/k_{-4} step. This postulation is supported by the observed sulfur elemental effect and complete loss of both polymerase and pyrophosphorolysis activities of D186 mutants.

Results obtained with the Klenow fragment by means of rapid kinetic techniques have identified two distinct nonchemical steps, before and after the phosphodiester bond formation (Kuchta et al., 1987; Dahlberg & Benkovic, 1991). The two steps before the bond formation are (i) initial binding of dNTP to E−DNA binary complex resulting in the formation of E−DNA−Mg·dNTP ternary complex (k_2) and (ii) subsequent conformational change of the ternary complex to a transition-state complex, E*−DNA−Mg·dNTP (k_3), that is poised for catalysis (see Figure 8). The transition-state complex undergoes rearrangement followed by phosphodiester bond formation (k_4). Similar to the two-step binding mechanism for dNTP, the existence of a two-step release mechanism for PP_i, where a conformational change of transition-state species E*−DNA_{n+1}−PP_i to ground-state species E−DNA_{n+1}−PP_i (k_5) and subsequent release of PP_i (k_6) has also been suggested (Dahlberg & Benkovic, 1991). Considering a similar reaction mechanism for HIV-1 RT (Reardon et al., 1992, 1993; Hsieh et al., 1993), the sulfur-sensitive step could be one of the two distinct steps k_3 and k_4 during the polymerase reaction. This sulfur-sensitive step may be the rate-limiting step for those carboxylate mutants which showed the elemental effect. This step may be the chemical step itself in which the phosphodiester bond is formed since a slower reaction rate with a sulfur−phosphate ester as compared with phosphate ester is considered to be a diagnostic indication for the chemical step as the rate-limiting step in the enzyme-catalyzed reaction (Eckstein, 1975; Polesky et al., 1992). However, lack of a significant elemental effect on the pre-steady-state rate of the polymerase reaction catalyzed by the wild-type HIV-1 RT (Hsieh et al., 1993; Reardon et al., 1992, 1993) exhibiting the same K_m for both dNTP and dNTPαS substrates (Pandey et al.,

unpublished results) has suggested that a step prior to the phosphate bond formation is rate-limiting for the nucleotide addition. Similar mechanism have been proposed for both the Klenow fragment (Mizrahi et al., 1985) and the T7 DNA polymerase (Patel et al., 1991). Recent evidence obtained by pulse−chase and pulse−quench experiments has suggested the existence of a slow nonchemical step as the rate-limiting step for HIV-1 RT which is attributed to a conformational change preceding the chemical step of the polymerase reaction (Hsieh et al., 1993). The lack of an elemental effect on the forward polymerase reaction (Hsieh et al., 1993; Reardon et al., 1992, 1993) of HIV-1 RT suggests that this nonchemical step is insensitive to sulfur substitution. Thus the high sensitivity to sulfur substitution seen with some of the carboxylate mutants in the present studies is indicative of the elemental effect influencing the chemical step of the reaction. Therefore, the elemental effects observed with the carboxylate mutants of HIV-1 RT, although highly complex, provided some basis for implicating the appropriate carboxylate in the chemical step of the reaction. For instance, D186A exhibited no elemental effect; D186E is extremely sensitive to sulfur substitution, showing drastically reduced incorporation rates of the phosphorothioate nucleotide, while D186N is actually stimulated with the sulfur substitution. Thus, these results can be explained on the basis of steric constraint imposed by the replacement of oxygen with the sulfur atom. Since the van der Waals radius of the sulfur atom is larger than that of the oxygen atom, the bond length between sulfur and phosphorus (1.94 Å) is also larger than that between oxygen and phosphorus (1.51 Å) (Eckstein, 1975). If P atom is considered as the center, then the effective radius of van der Waals surface mapped by the oxygen and sulfur atoms will be 2.9 and 3.7 Å, respectively. The limited volume in the active site of the enzyme may be responsible for the reduction in the turnover of the thio-substituted dNTPs. Since dNTPαS (S_p isomer) contains a sulfur atom in the double-bond configuration (P═S), coordination with the metal ion is not affected, and therefore at the k_2 step, both dNTP and dNTPα S bind to the active site of the E−DNA binary complex with equal affinity (Burgers et al., 1979). However, in the transition state during phosphodiester bond formation (k_4), two major events take place. First, the tetravalent phosphorus becomes pentavalent, and second, an inversion of the configuration occurs during the chemical step. In both or either of the two steps, the bulky nature of sulfur may produce a steric clash with the surrounding atoms, resulting in slowing down the rate of the corresponding step of the reaction. The differing and opposite elemental effect ensuing from D → A, D → E, and D → N substitution at Asp 186 can be explained by correlating with the length of the side chain (D186A → D186E → D186N). This parity suggest that the steric hindrance is absent with the smaller side chain of Ala, aggravated by a longer side chain of Glu, but relieved by substitution with an equal length side chain of Asn, resulting in stimulation (as compared to D → E) of the reaction. It was further observed that incorporation of multiple sulfur nucleotides slightly increased the binding affinity for the template−primer (Figure 5). Therefore, the stimulation of incorporation of phosphorothioate nucleotide versus normal nucleotide noted with the D186N mutant may also be partly due to this primer effect. These results strongly suggest that, in the transition-state ternary complex (k_4), residue D186 may be proximal to the α-phosphoryl group of Mg·dNTP and it may be involved in the polarization of the nucleophile at the phosphodiester bond formation step (k_4). The failure of D186 mutants to catalyze the reverse polymerase (pyrophosphorolysis) reaction provides a further suggestion that the same residue may play a catalytic role in the chemical step of both the forward and the reverse reactions. D110 mutants were also devoid of pyrophosphorolysis reaction, which could be attributed to their inability to bind the PP_i substrate. Ability of D185 mutants to catalyze the pyrophosphorolysis reaction suggest that D185 may not be the catalytic residue for the reverse reaction although it is crucial for the forward reaction.

The analyses of the biochemical properties of individual aspartate mutants of HIV-1 RT should be helpful in defining the geometry of the ternary complex as well as that of the transition-state complex. Since a three-dimensional molecular model structure of enzyme−DNA−Mg·dNTP ternary complex of HIV-1 RT is available (Pandey et al., 1996), we used this model to analyze these biochemical data in 3-D context to assign the possible role of the individual carboxylates in the polymerization reaction (Figure 9). In the ternary complex, the position of the Pα atom was aligned at approximately 3 Å distance from the 3′-O of the primer terminus to fulfill the SN_2 nucleophilic addition reaction criteria and β- and γ-phosphates at an interacting distance (through Mg^{2+}) from the oxygens of the catalytic carboxylate triad, D110, D185, and D186. We propose that the initial binding of dNTP (k_2/k_{-2}) takes place *via* D186 and D110 by coordination with $\beta-\gamma$-phosphate through metal B followed by alignment of the 3′-OH of the primer terminus and Pα of dNTP through coordination with metal A and all three carboxylates.

In the transition state, which is accompanied by a change from tetrahedral geometry of the Pα to trigonal bipyramidal geometry as well as inversion of configuration at Pα (Burgers & Eckstein, 1978), Asp 186 seems to be most critical due to its axial configuration opposite the O of Pα (Figure 10). The large sulfur elemental effect seen with the mutants of D186 supports this postulation. The reversal of this reaction (pyrophosphorolysis) could also be facilitated under this situation where Pα of dNTP has now become a diester phosphate of the ultimate primer nucleotide. Noninvolvement of D185 in the pyrophosphorolysis reaction, where 3′-O has no role to play, supports this premise. The other metal ion coordinating with D110 may stabilize the negative charges on the $\beta-\gamma$-phosphate of dNTP at the k_3/k_{-3} step and on PP_i at the k_5/k_{-5} step.

The structure of the transition state of the phosphoryl transfer reaction is expected to be common for the forward (polymerization) as well as for the reverse (pyrophosphorolysis) reaction. The mutants of those carboxylates that participate in the transition-state binding (as opposed to the ground-state dNTP binding) would exhibit an identical effect in both forward and reverse reactions. On the other hand, an isolated effect on one of the two reactions (e.g., polymerization and not pyrophosphorolysis) should be interpreted as participation of this residue in a step preceding the formation of the transition state, such as initial dNTP binding (k_2/k_{-3} step). D185 seems to be a residue of the latter type, probably binding the incoming dNTP through metal A at the early stage of the reaction. After the proposed conformational change (k_3) (Reardon et al., 1992, 1993; Hsieh et

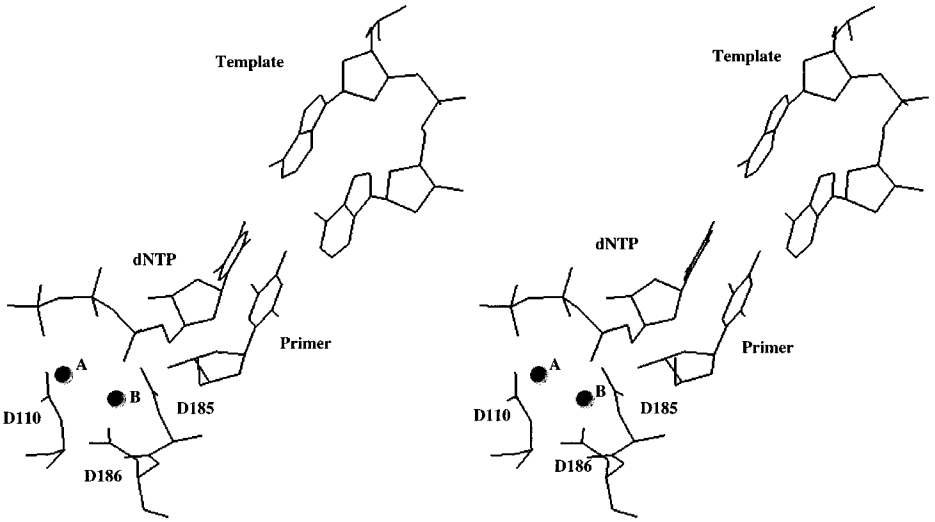

FIGURE 9: Molecular model of the pre-transition-state ternary complex of HIV-1 RT showing the suggested interaction of the catalytic carboxylate triad. The entire backbone structure of HIV-1 RT is based on the only available DNA-bound HIV-1 RT crystal structure (PDB file 1HMI; Jacobo-Molina et al., 1993). Modeling of the complete structure including the side chains was performed using the SYBYL molecular modeling package as described before (Yadav et al., 1992, 1995). To model a template−primer, we generated a duplex DNA in the A form comprising the AAA/TT sequence using the algorithm of Arnott and Hukins (1972). Both HIV-1 RT and the template−primer structures were energy-refined. Docking of template−primer into the HIV-1 RT structure was done by superimposing P-atoms of the modeled DNA onto the P atom position in the RT-DNA crystal structure (Jacobo-Molina et al., 1993). The position of dTTP into the RT−DNA model was fixed by creating a Watson−Crick base pair between the base moiety of dTTP and template nucleotide. The position of Pα with respect to the 3′-O of the primer terminus was aligned to fulfill the SN_2 nucleophilic addition reaction criteria. The metal coordination position in the triphosphate moiety of dTTP was derived from the crystal structure of the rat DNA polymerase−β-DNA−dNTP ternary complex (Pelletier et al., 1994). The geometry of the ternary complex was minimized using the MAXIMIN2 minimizer and the Kollman united force field approach (Weiner et al., 1984). In the resulting prepolymerase ternary complex, Pα is seen at approximately 3 Å distance from the 3′-O of the primer terminus and β- and γ-phosphates at an interacting distance (through Mg^{2+}) from the oxygens of the catalytic carboxylate triad, D110, D185, and D186. The Mg^{2+} ions are shown as two closed circles. In this complex Asp 185 is shown to coordinate with metal A, while Asp 186 and Asp 110 coordinate with both the metal ions A and B. Initial binding of dNTP occurs through the β−γ-phosphate via metal B and Asp 186 and Asp 110. Alignment of the 3′-OH of the primer terminus with respect to Pα in a linear fashion is maintained by Asp 185 and Asp 186.

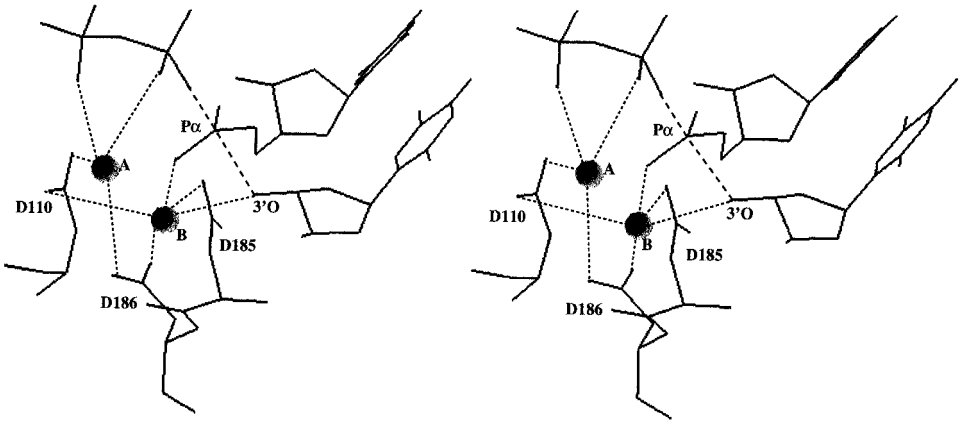

FIGURE 10: Transition-state ternary complex of HIV-1 RT. This structure is derived from the prepolymerase ternary complex structure as shown in Figure 9. In this transition-state complex, Asp 186 is directly coordinating to the Pα oxygen through metal A. The positions of the Pα oxygen, metal A, and carboxylate oxygen of Asp 186 are axial, and the distance between metal A and the oxygen (O) atom of Asp 186 is the lowest among other coordination sites. This transition-state structure is also relevant for the reverse reaction where Pα of dNTP has now become the diester phosphate of the ultimate primer nucleotide. This indicates that Asp 186 is the most crucial residue in maintaining the stabilization of pentavalent Pα geometry in the transition state in both forward (polymerase) and reverse (pyrophosphorolysis) reactions. This is in agreement with our experimental observation that the mutants of Asp 186 exhibit a large sulfur elemental effect and are also devoid of pyrophosphorolysis activity. Broken lines (- - -) indicate the bond formation/cleavage and dotted lines (···) indicate the metal coordination.

al., 1993) and the initiation of the bond formation and cleavage process (k_4/k_{-4}), D185 may not be playing a critical role in coordinating with metal A. This is evident from our finding that mutants of D185 have significant pyrophosphorolysis activity, suggesting that it is not directly participating in the stabilization of the transition-state complex. Instead, as shown in the model (Figure 10), D185 may be interacting directly with the 3′-OH of the primer, acting as a proton acceptor in a general base mechanism. Interestingly, the 3′OH−D185 interaction is absent in pyrophosphorolysis (lack of 3′−OH); hence, D185 is not required for this reaction. In contrast to D185, we propose the involvement of other two residues (D110 and D186) of the catalytic triad in the stabilization of the transition state of the reaction.

In summary, we have obtained information regarding binding of dNTP wherein all three carboxylates participate in the initial binding of the Mg·dNTP, and subsequently only D186 and D110 go on to stabilize the transition state of the

reaction. Further exploration of the transition state is expected to provide insight regarding the reaction mechanism in general and the precise role of specific residues in particular. The transition-state structure of HIV-1 RT and the residues involved in stabilizing this state may also be highly relevant for the design of transition-state analog inhibitors.

REFERENCES

Arnott, S., & Hukins, D. W. L. (1972) *Biochem. Biophys. Res. Commun. 47*, 1504−1511.

Ausubel, F. M, Brent, R., Kingston, R. E., Moore, D. D., Seidman, J. S., Smith, J. A., & Struhl, K. (1987) *Current Protocols in Molecular Biology*, Greene Publishing Associates and Wiley−Intersciences, John Wiley & Sons, New York.

Barre-Sinoussi, F., Cherman, J. C., Rey, F., Nugeyre, M. T., Chamaret, S., Gruest, J., Dauguet, C., Axler-Bin, C., Vezinet-Brun, F., Rouzioux, C., Rosenbaum, W., & Montagnier, L. (1983) *Science 220*, 868−871.

Boyer, P. L., Ferris, A. L., & Hughes, S. H. (1992) *J. Virology 66*, 1031−1039.

Boyer, P. L., Ferris, A. L., Clark, P., Whitmer, J., Frank, P., Tantillo, C., Arnold, E., & Hughes, S. H. (1994) *J. Mol. Biol. 243*, 472−483.

Bryant, F. R., Johnson, K. A., & Benkovic, S. J. (1983) *Biochemistry 22*, 3537−3546.

Burgers, P. M. J., & Eckstein, F. (1978) *Proc. Natl. Acad. Sci. U.S.A. 75*, 4798−4800.

Burgers, P. M. J., & Eckstein, F. (1979) *J. Biol. Chem. 254*, 6889−6893.

Dahlberg, M. E., & Benkovic, S. J. (1991). *Biochemistry 30*, 4835−4843.

Desai, S. D., Pandey, V. N., & Modak., M. J. (1994) *Biochemistry 33*, 11868−11874.

DiMarzo-Veronese, F., Copeland, T. D., DeVico, A. L., Rahman, R., Oroszlan, S., Gallo, R. C., & Sarangadharan, M. G. (1986) *Science 231*, 1289−1291.

Eckstein, F. (1975) *Angew. Chem., Int. Ed. Engl. 114*, 160−166.

Hansen, J., Schulze, T., & Moelling, K. (1987) *J. Biol. Chem. 262*, 12393−12396.

Hostomsky, Z., Hostomska, Z., Fu, T. B., & Taylor, J. (1992) *J. Virol. 66*, 3179−3182.

Hsieh, J. C., Zinnen S., & Modrich, P. (1993) *J. Biol. Chem. 268*, 24607−24613.

Jacobo-Molina, A., Ding, J., Nanni, R. G., Clark, A. D., Lu, X., Tantillo, C., Williams, R. L., Kamer, G., Ferris, A. L., Clark, P., Hizi, A., Hughes, S. H., & Arnold, E. (1993) *Proc. Natl. Acad. Sci. U.S.A. 90*, 6320−6324.

James, E., & Morrison, J. F. (1966) *J. Biol. Chem. 241*, 4758−4770.

Kati, W. M., Johnson, K. A., Jerva, L. F., & Anderson, K. S. (1992) *J. Biol. Chem. 267*, 25988−25997.

Kohlstaedt, L. A., Wang, J., Friedman, J. M., Rice, P. A., & Steitz, T. A. (1992) *Science 256*, 1783−1790.

Kuchta, R. D., Mizrahi, V., Benkovic, P. A., Johnson, K. A., & Benkovic, S. J.(1987) *Biochemistry 26*, 8410−8417.

Kunkel, T. A., Roberts, J. D., & Zakour, R. A. (1987) *Methods Enzymol. 154*, 367−382.

Larder, B. A., Kemp, S. D., & Purifoy, D. J. M (1989) *Proc. Natl. Acad. Sci. U.S.A. 86*, 4803−4807.

Larder, B. A. (1993) *Reverse Transcriptase* (Skalka, A. M., & Goff, S. P., Eds.) pp 205−222, Cold Spring Harbor Laboratory Press, Cold Spring Harbor, NY.

Larder, B. A., Purifoy, D. J. M., Powell, K. L., & Darby, G. (1987) *Nature 327*, 716−717.

LeGrice, S. F. J., Naas, T., Wohlgensinger, B., & Schatz, O., (1991) *EMBO J. 10*, 3905−3907.

Leuthardt, A., & Le Grice, S. F. J.(1988) *Gene 68*, 35−42.

Levy, J. A., Hoffman, A. D., Kramer, S. M., Landis, J. A., Shimabukuro, J. M. & Oshiro, L. S. (1984) *Science 225*, 840−842.

Lightfoote, M. M., Coligan, J. E., Folks, T. M., Fauci, A. S., Martin, M. A., & Venkatesan, S. (1986) *J. Virol. 60*, 771−775.

Lowe, D. M., Parmar, V., Kemp, S. D., & Larder, B. A. (1991) *FEBS Lett. 282*, 231−234.

Majumdar, C., Abbotts, J., Broder, S., & Wilson, S. H. (1988) *J. Biol. Chem. 263*, 15657−15665.

Majumdar, C., Stein, C. A., Cohen, J. S., Broder, S., & Wilson, S. H. (1989) *Biochemistry 28*, 1340−1346.

Maxam, A., & Gilbert, W. (1980) *Methods Enzymol. 65*, 499−560.

Mizrahi, V., Henrie, R. N., Marlier, J. F., Johnson, K. A., & Benkovic, S. J. (1985) *Biochemistry 24*, 4010−4018.

Mous, J., Heimer, E. P., & Le Grice, S. F. J. (1988) *J. Virol. 62*, 1433−1436.

Pandey, V. N., & Modak, M. J. (1987a) *Biochemistry 26*, 2033−2038.

Pandey, V. N., & Modak, M. J. (1987b) *Prep. Biochem. 17*, 359−377.

Pandey, V. N., & Modak, M. J. (1988) *J. Biol. Chem. 263*, 3744−3751.

Pandey, V. N. William, K. R. Stone, K. L., & Modak, M. J. (1987) *Biochemistry 26*, 7744−7748.

Pandey, V. N., Kaushik, N., & Modak, M. J. (1994a) *J. Biol. Chem. 269*, 13259−13265.

Pandey, V. N., Kaushik, N., & Modak, M. J. (1994b) *J. Biol. Chem. 269*, 21828−21834.

Pandey, V. N., Kaushik, N., Rege, N. Sarafianos, S. G., Yadav, P. N. S., & Modak, M. J. (1996) *Biochemistry 35*, 2168 −2179.

Patel, S. S., Wong, I., & Johnson, K. A. (1991) *Biochemistry 30*, 511−525.

Patel, P. H., Jacobo-Molina, A., Ding, J., Tantillo, C., Clark, A. D., Rag, R., Nani, R. G., Hughes, S., & Arnold, E. (1995) *Biochemistry 34*, 5351−5363.

Pelletier, H. (1994) *Science 266*, 2025−2026.

Pelletier, H., Sawaya, M. R., Kumar, A., Wilson, S. H., & Kraut, J. (1994) *Science 264*, 1891−1903.

Polesky, A. H., Dahlberg, M. E., Benkovic, S. J., Grindley, N. D. F., & Joyce, C. M. (1992) *J. Biol. Chem. 267*, 8417−8428.

Popovic, M., Sarangadharan, M. G., Read, E., & Gallo, R. C. (1984) *Science 224*, 497−500.

Reardon, J. E. (1992) *Biochemistry 31*, 4473−4479.

Reardon, J. E. (1993) *J. Biol. Chem. 268*, 8743−8751.

Sarafianos, S. G., Pandey, V. N., Kaushik, N., & Modak, M. J. (1995a) *Biochemistry 34*, 7207−7216.

Sarafianos, S. G., Pandey, V. N., Kaushik, N., & Modak, M. J. (1995b) *J. Biol. Chem. 270*, 19729−19735.

Steitz, T. A., Smerdon, S., Jäger, J., & Joyce, C. M. (1994) *Science 266*, 2022−2025.

Wakefield, J. K., Jblonski, S. A., & Morrow, C. D. (1992) *J. Virol. 66*, 1031−1039.

Weiner, S. J., Kollman, P. A., Case, D. A., Singh, U. C., Ghio, C., Altona, G., Profeta, S., & Weiner, J. (1984) *J. Am. Chem. Soc. 106*, 765−784.

Yadav, P. N. S., Yadav, J. S., Arnold, E., & Modak, M. J. (1994) *J. Biol. Chem. 269*, 716−720.

Yadav, P. N. S., Yadav, J. S., & Modak, M. J. (1995) *Nature Struct. Biol. 2*, 193−195.

BI960364X